Pressure-Induced Reactivity in the Emeraldine Salt and Base Forms of Polyaniline Probed by FTIR and Raman

ARTICLE *in* THE JOURNAL OF PHYSICAL CHEMISTRY C · NOVEMBER 2014

Impact Factor: 4.77 · DOI: 10.1021/jp509154j

4 AUTHORS, INCLUDING:

Marcelo Medre Nobrega
University of São Paulo
27 PUBLICATIONS **105** CITATIONS

SEE PROFILE

THE JOURNAL OF PHYSICAL CHEMISTRY C

Article

pubs.acs.org/JPCC

Pressure-Induced Reactivity in the Emeraldine Salt and Base Forms of Polyaniline Probed by FTIR and Raman

Marcelo M. Nobrega,[†,‡] Matteo Ceppatelli,[‡,§] Marcia L. A. Temperini,[*,†] and Roberto Bini[‡,∥]

[†]Departamento de Química Fundamental, Instituto de Química da Universidade de São Paulo (USP), C.P. 26077- CEP 05513-970 - São Paulo, SP, Brazil

[‡]LENS, European Laboratory for Nonlinear Spectroscopy, Via Nello Carrara 1, 50019 Sesto Fiorentino (FI), Italy

[∥]Dipartimento di Chimica "Ugo Schiff" dell'Università degli Studi di Firenze, Via della Lastruccia 3, 50019 Sesto Fiorentino (FI), Italy

[§]ICCOM-CNR, Institute of Chemistry of OrganoMetallic Compounds, National Research Council of Italy, Via Madonna del Piano 10, I-50019 Sesto Fiorentino, Firenze, Italy

Supporting Information

ABSTRACT: This report presents the influence of the morphology on the pressure-induced reactivity of the doped (PANI-ES) and dedoped (PANI-EB) forms of polyaniline using Raman and FTIR techniques. Our PANI-EB FTIR spectroscopy data showed an intensity exchange among characteristic bands of the quinoid and benzoic segments above 9 GPa, suggesting a specific coupling reaction between adjacent quinoid rings. The reaction kinetic was followed, and the results showed a dependence of the rate constant with pressure, as well as the activation volume, presented an inversion from negative to positive at 13 GPa, suggesting that steric factors have a role in the reactivity of the species. Raman spectra of PANI-ES showed a broadening and a blue shift of the bands as the pressure increases preceding the almost complete amorphization of the polymer; after decompression, some minor spectral changes were observed, suggesting the occurrence of the dedoping and cross-linking reactions in less extension than PANI-EB.

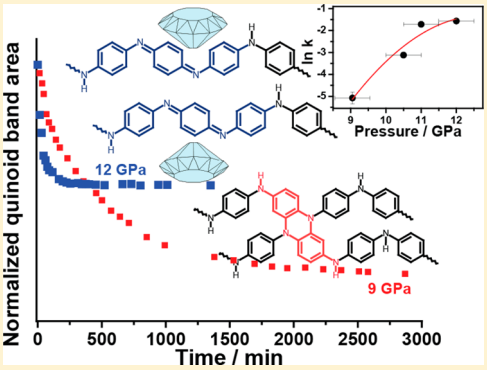

INTRODUCTION

High pressure research field has emerged as a new and independent research area since the pioneering work of Bridgman[1] and with the advent of the diamond anvil cell (DAC).[2] High pressures in the GPa range are capable of tuning the intermolecular/interatomic distances of the system thus increasing its energy. As a consequence, the responses of the system to these severe changes of the intermolecular distances and to the accumulation of energy are the rearrangements of the molecular conformation and the modification of the chemical bonds, resulting in a number of phenomena including phase transitions, ionization, amorphization, and dissociation.[3−7]

Remarkable high pressure studies were reported in the literature in the last years such as high pressure photoinduced ring opening in benzene,[8] evidence for high pressure polymorphism in resorcinol,[9] high pressure dimerization of butadiene,[10] and many others.[11−18] Most parts of these studies were performed in simple systems, however, one of the most important fields in chemistry is the materials chemistry, specifically, the conducting polymers. Among the conducting polymers, polyaniline (PANI) is fascinating material due to its mechanical, optical, and electronic properties,[19,20] which open to potential applications in several devices, including microelectronics, electrochromic displays, and secondary batteries.[20−28]

Recently, nanostructured PANI has been extensively studied, particularly PANI nanofibers are of great interest since they combine high surface area and low dimensionality presenting better performance than bulk PANI in several devices such as chemical sensors, solid-state batteries, solar cells, electronic or electrochromic devices and antistatic coating.[27,29−31] Nevertheless, little has been done in the high pressure research field having PANI as subject,[32,33] such as, the dependence of the resistance of bulk PANI, the electrical conductivity, and the FTIR spectra as a function of pressure, studied in the late 90s.[34−36]

It is well-known that vibrational techniques are very powerful tools in the structural study of PANI. Resonance Raman (RR) spectroscopy is useful to study and characterize different oxidation and doping forms of PANI, and it is also used in the characterization of several chromophoric groups resulting from the cross-linking reactions between the PANI chains.[37−44]

This report investigates the effect of the morphology in the behavior of the doped and dedoped forms of PANI during the

Received: September 10, 2014
Revised: October 13, 2014

   dx.doi.org/10.1021/jp509154j | J. Phys. Chem. C XXXX, XXX, XXX−XXX

compression−decompression cycle up to 15 GPa. The structural modifications were monitored through Raman and infrared spectroscopies. Our FTIR spectroscopy data of PANI-EB showed that above 9 GPa a decrease in the intensity of the band due to the quinoid segments and an increase in the band of the benzoid segments occurs, suggesting a specific cross-linking reaction. The reaction kinetics at four pressures was followed and the results showed a dependence of the rate constant with pressure. It was observed an inversion in the activation volume sign from negative at 9 GPa to positive at 14 GPa, suggesting that increasing pressure, the hindrance of the system increases and the reaction occurs only in specific sites formed during the compression of the system. From the results presented herein, it was possible to conclude that morphology played no important role in the behavior of the polymer, since the reaction threshold was the same for the polymers with bulk and fiber morphology. Raman spectra of PANI-ES showed some minor spectral changes after the decompression of the system which suggested the occurrence of the dedoping and cross-linking reactions.

EXPERIMENTAL SECTION

Aniline monomer ($C_6H_5NH_2$, Merck) was distilled under reduced pressure prior to use. Ammonium peroxydisulfate $(NH_4)_2S_2O_8$ (Merck) and HCl (Sigma-Aldrich, 37%) were used as received.

Synthesis of Polyaniline Emeraldine Salt and Base with Bulk Morphology. Polyaniline bulk in emeraldine salt form (denoted as "PANI-ES-bulk") was prepared by the usual well know route through the chemical oxidative polymerization of aniline with ammonium peroxydisulfate (APS) in 1 mol L^{-1} hydrochloric acid at about 5 °C during 1 h (monomer/oxidant molar ratio of ca. 4/1).[45] The concentrations of aniline and APS solutions were about 0.73 and 0.25 mol L^{-1}, respectively. The dark green precipitate was isolated by filtration, washed with 250 mL of 1 mol L^{-1} hydrochloric acid and dried under reduced pressure at room temperature. Polyaniline powder in emeraldine base form (denoted as "PANI-EB-bulk") was prepared by dedoping of 150 mg of ES-powder in 150 mL of 0.1 mol L^{-1} NH_3 solution during 15 h. The solid was isolated by filtration and treated again with 150 mL of 0.1 mol L^{-1} NH_3 solution for 1 h. The dark blue solid was filtered, washed with 150 mL of 0.1 mol L^{-1} NH_3 solution, and dried under reduced pressure at room temperature.

Synthesis of Nanofibers of Polyniline through Rapid Mixing Synthesis (PANI-RM). Nanofibers of polyaniline in the emeraldine salt form were synthesized by rapid mixing reaction (denoted as "PANI-ES-RM").[46] An aqueous solution of aniline 0.56 mL (3.2 mmol) was dissolved in 20 mL of 1.0 mol L^{-1} HCl and another solution of ammonium peroxydisulfate (APS) dissolving 1.6 g (0.8 mmol) of APS in 20 mL of 1.0 mol L^{-1} HCl were prepared. The rapid mixing reaction was carried out by pouring the two solutions together under vigorous stirring in order to ensure the uniformity of the mixture before the polymerization begins. The polymerization was observed when the characteristic green color of polyaniline in the emeraldine salt form became visible (ca. 7 min). The dark green solid was isolated by centrifugation at 7000 rpm during 15 min and the supernatant was changed by a new aqueous solution of HCl 1.0 mol L^{-1}, this process was repeated three times and the solid was dried under vacuum at room temperature. PANI nanofibers in emeraldine base form (denoted as PANI-EB-RM) was prepared by dedoping of 150 mg of PANI-ES-RM nanofibers in 150 mL of 0.1 mol L^{-1} NH_3 solution during 15 h. The solid was isolated by centrifugation at 7000 rpm during 15 min and the supernatant was changed by a new solution of 0.1 mol L^{-1} NH_3 this process was repeated three times. The dark blue solid was filtered, washed with 150 mL of 0.1 mol L^{-1} NH_3 solution and dried under reduced pressure at room temperature.

Synthesis of Emeraldine Base and Salt Forms of PANI Nanofibers Using Interfacial Polymerization (PANI-IF). PANI nanofibers in emeraldine salt form (denoted as "PANI-ES-IF") were prepared by the interfacial polymerization aniline by ammonium peroxydisulfate (APS), described in ref 37, in acidic aqueous phase. In an interfacial polymerization, two solutions were prepared separately: (i) 5 mL of aniline (54.9 mmol) was dissolved in 200 mL of chloroform (organic solution); (ii) 3.13 g of APS (13.7 mmol) was dissolved in 300 mL of aqueous solution of HCl 1.0 mol L^{-1}(aqueous solution). The aqueous solution (ii) was slowly added to the organic solution (i), and the system was kept at room temperature during 24 h. After this period, the aqueous phase containing PANI nanofibers was centrifuged at 7000 rpm during 15 min and the supernatant was changed by a new aqueous solution of HCl 1.0 mol L^{-1}, this process was repeated three times and the solid was dried under vacuum at room temperature. PANI nanofibers in emeraldine base form (denoted as PANI-EB-IF) was prepared by dedoping of 150 mg of PANI-ES nanofibers in 150 mL of 0.1 mol L^{-1} NH_3 solution during 15 h. The solid was isolated by centrifugation at 7000 rpm during 15 min, and the supernatant was changed by a new solution of 0.1 mol L^{-1} NH_3; this process was repeated three times. The dark blue solid was filtered, washed with 150 mL of 0.1 mol L^{-1} NH_3 solution, and dried under reduced pressure at room temperature.

Characterization Techniques. Samples for the Raman measurements of the doped (PANI-ES) and dedoped (PANI-EB) forms of PANI with morphologies bulk and fibers were loaded into a membrane diamond anvil cell (MDAC) by filling the gasket hole. The MDAC cell was equipped with IIa type diamonds and a stainless steel gasket. The gaskets were indented to a desired thickness (50−70 μm) and then a 150 μm diameter hole was drilled in the center of the indented region by the spark-erosion technique. A small ruby chip was placed on the sample for the in situ pressure measurements by the R_1 ruby fluorescence band shift method[47] and argon used as pressure transmitting medium since it is quasi hydrostatic up to 15 GPa. In order to ensure that there were no changes in temperature during pressure increase, the temperature of the sample was monitored during the experiment by a Si-diode placed on the metal gasketing the sample.

In order to obtain a homogeneous thin film for the FTIR measurements the samples of PANI-EB were prepared according to the following procedure. A small grain of sample was placed in the center of the upper diamond the cell was closed squeezing the sample between the diamonds, after this the cell was reopened and an excess of sample was removed of the upper diamond leaving sample only in the center of the diamond, the procedure was repeated until obtaining a homogeneous thin film in the center of the diamond. The gasket was then placed on the lower diamond, a small ruby chip was placed inside the gasket hole, and the sample volume was filled by liquid argon.

FTIR absorption measurements recorded with an instrumental resolution of 1 cm^{-1} were performed with a Bruker-IFS 120 HR spectrometer modified for high-pressure measure-

dx.doi.org/10.1021/jp509154j | J. Phys. Chem. C XXXX, XXX, XXX−XXX

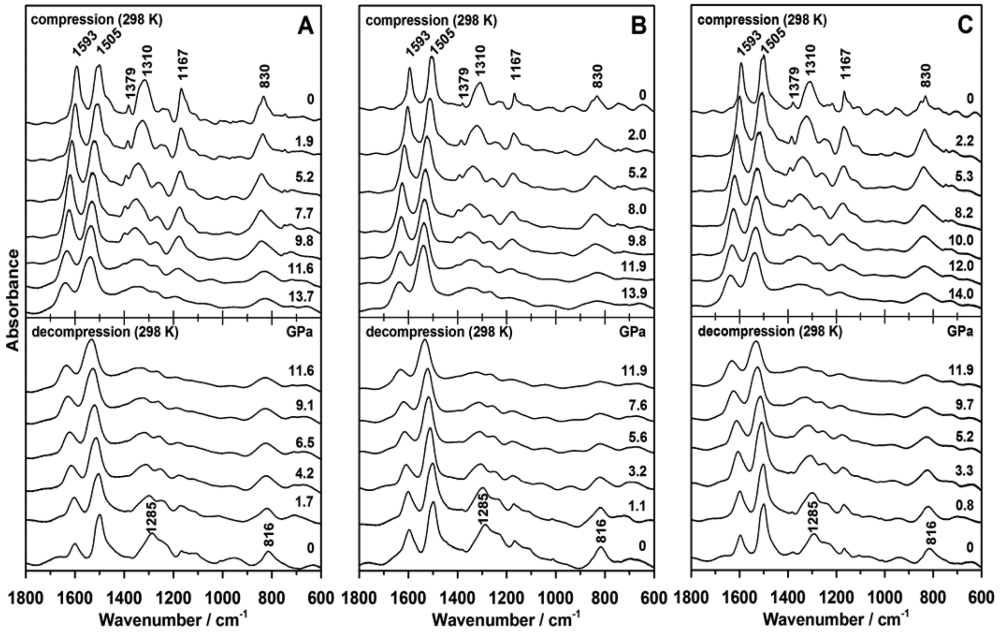

Figure 1. FTIR spectra of (A) PANI-EB-bulk, (B) PANI-EB-IF, and (C) PANI-EB-RM for selected pressures recorded during the compression (upper panels) and decompression (lower panels) at 298 K. PANI-EB-bulk is the polymer with granular morphology, PANI-EB-IF is the polyaniline with nanofiber morphology obtained through the interfacial polymerization[37] and PANI-EB-RM is the polyaniline with nanofiber morphology obtained through the rapid mixing polymerization.[46]

ments. The ruby fluorescence was excited using few milliwatts of a 532 nm laser line from Nd:YAG laser source. Raman spectra were measured in a backscattering geometry by using the 647.1 nm line of a Kr+ laser with a laser power ranging from 1 to 10 mW, the scattered light was dispersed by a single-stage monochromator (900 grooves/mm) and analyzed by a CCD detector a resulting instrumental resolution of 0.7 cm^{-1}, the acquisition time were 600 s.

RESULTS AND DISCUSSION

The dedoped form of PANI (PANI-EB), both with bulk and fiber morphology, were analyzed using FTIR spectroscopy and Raman techniques. However, the FTIR spectroscopy experiments were by far more informative about its behavior under high-pressure than Raman technique. The doped form of PANI (PANI-ES) was analyzed only through Raman spectroscopy due to the instability of the polymer during the preparation of thin films for the FTIR spectroscopy experiments which were mandatorily required because of its strong absorbance in the NIR region.[48−52] For the sake of clarity, the FTIR spectroscopy and Raman results are presented in separated sections.

FTIR Spectra. A high stability of PANI-EB was observed under pressure for both bulk and fiber morphologies. The FTIR spectra as a function of pressure at room temperature were obtained in step of 1 GPa during a compression−decompression cycle up to 15 GPa, Figure 1. The characteristic bands of PANI-EB at ambient pressure are due to the quinoid segments at 1593 ($\nu_{C=C(Q)}$), 1505 ($\nu_{C-C(B)}$), 1379 ($\nu_{C-C(Q)}$), 1310 ($\beta_{C-H(Q)} + \beta_{C-H(B)}$), 1167 ($\beta_{C-H(B)}$), and 830 ($\beta_{C-H\ o.p.\ (B)}$ + ring. $def._{(Q)}$) cm^{-1}.[53]

As the pressure is increased, a broadening and blue shifts of the bands precede the complete loss of the spectral signatures possibly indicating a partial or complete amorphyzation of the polymer observed above 14 GPa. Under the decompression step, it is clearly observed that the amorphization is almost completely reversible and the recovered spectrum is very similar to the starting one unless a broadening of the bands. However, some differences are noticed in the recovered spectrum, a decrease in the intensity of the band at 1595 cm^{-1}, the band at 1379 cm^{-1} completely disappeared, the band at 1310 was shifted to 1285 cm^{-1} and the band at 830 was shifted to 816 cm^{-1}. According to the vibrational analysis of the infrared spectrum of PANI-EB, it is known that the band at 1310 ($\beta_{C-H(Q)} + \beta_{C-H(B)}$) and 830 (ring. $def._{(Q)} + \beta_{C-H\ o.p.\ (B)}$) cm^{-1} presents the contribution of both quinoid and benzoid segments, and the component with the high frequency is associated with the quinoid segments.[53] The shift to lower frequency of these bands in the recovered spectrum is consistent with a decrease-disappearance in the contribution of the quinoid components.

Zeng et al.[36] reported a similar behavior for PANI-EB chemically synthesized using potassium dichromate as oxidant. In this study, the weakening of the bands at about 1390 cm^{-1} and at 1590 cm^{-1} was reported when the pressure was increased above 3.9 GPa, suggesting a decrease in the amount of quinoid units. This occurrence was ascribed to a poor structural stability of the quinoid segments. It is important to notice that the band at 1505 cm^{-1}, due to the benzoid segments, persists with high relative intensity at 14 GPa and in the recovered spectrum. This result could suggest that under high pressure the polymer chains tend to organize in a way that the amount of benzenoid rings increases to the expense of quinoid rings.

In order to verify the behavior of the quinoid and the benzoid rings in PANI-EB chains as a function of pressure, the areas of the bands at 1593 (quinoid) and 1505 (benzoid) cm^{-1} were integrated and the intensity ratio (I_{1593}/I_{1505}) was plotted as a function of pressure during the compression−decompression cycle at 298 K, Figure 2A. During the compression cycle two patterns are distinguishable: the first from ambient pressure up to 9 GPa where the intensity ratio (I_{1593}/I_{1505}) remains practically unaltered; the other from 9 to 15 GPa

dx.doi.org/10.1021/jp509154j | J. Phys. Chem. C XXXX, XXX, XXX−XXX

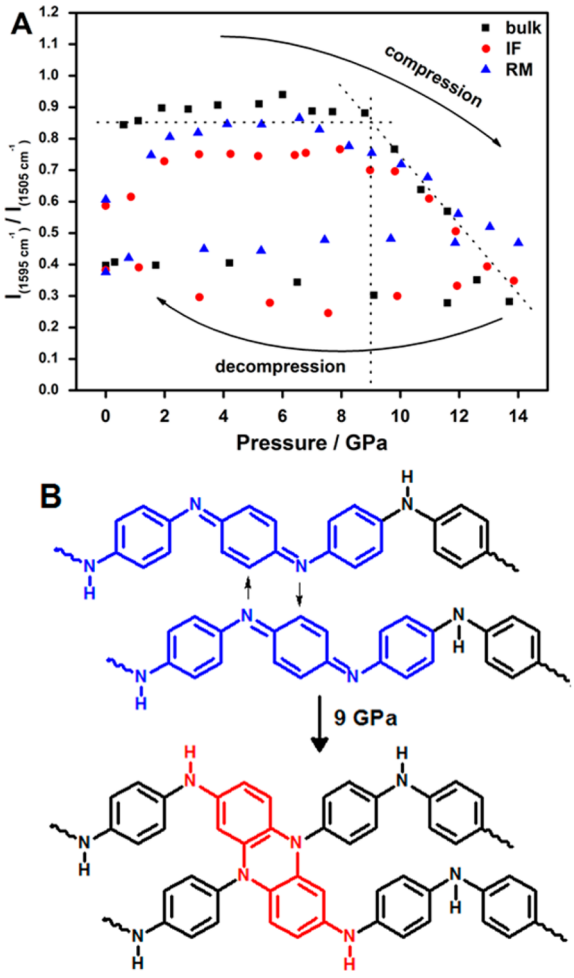

Figure 2. (A) Intensity ratio (I_{1593}/I_{1505}) of the integrated area of the bands at 1593 and 1505 cm^{-1} of PANI-EB with bulk and fiber morphology during the compression−decompression cycle at 298 K. (B) Cross-linking reaction driven by pressure for PANI-EB. Adapted from refs 37, 39, and 40.

where a decrease in the intensity ratio is observed. According to Figure 2A, 9 GPa is the pressure threshold in which the interaction between the quinoid rings is strong enough to start a coupling reaction between two adjacent quinoid rings, schematically represented in Figure 2B. The same reaction mechanism for PANI-EB was already reported in the literature considering the heating treatment of the polymer.[40] Our results suggest that the same specific cross-linking reaction is occurring through the coupling of the imine nitrogens to the quinoid rings of two adjacent quinoid segments, resulting in a nonaromatic three rings segment which is a metastable form at ambient pressure. Finally, it is possible to conclude from the results presented in Figures 1 and 2A that despite the difference in the supramolecular morphology, bulk and fiber, the arrangement of the chains in both morphologies did not influenced the behavior of the polymer under extreme high pressure conditions, up to 15 GPa.

The frequency shifts as a function of pressure of eight of the internal modes in the 800−1700 cm^{-1} frequency range shown in Figure 1 did not exhibit any discontinuity that could suggest changes in the chain packing, Figure 3. The pressure shifts of all modes were nearly linear with slopes ranging between 0.8 and 4 cm^{-1}/GPa. From these plots and the changes noticed in the FTIR spectra during the compression−decompression cycle, it is possible to conclude that no major changes are occurring between PANI chains under high pressure besides the coupling reaction among two quinoid rings discussed above.

Reaction Kinetics. Considering that there are no differences in the behavior of the polymer due to its morphologies with the pressure, only the kinetics reaction of PANI-EB-IF was followed at four different pressures (9.0, 10.5, 11.1, and 12.0 GPa) at 298 K. As stressed above, the reaction kinetics of the quinoid ring coupling was followed by the intensity decrease of the quinoid band at 1593 cm^{-1}. The evolution of the integrated area of the quinoid segments band as a function of time at constant pressure is reported in Figure 4A. According to the proposed reaction mechanism presented in Figure 2B, it is expected that the reaction will follow a second order kinetic law if two chains are involved in the coupling mechanism. Therefore, the data were fitted by eq 1.

$$A_{(t)} = \frac{A_0}{A_0 kt + 1} \tag{1}$$

where k is the rate constant and A_0 and $A_{(t)}$ is the integrated absorbance at initial time and at time t, respectively. The fit is excellent for all the reaction pressures.

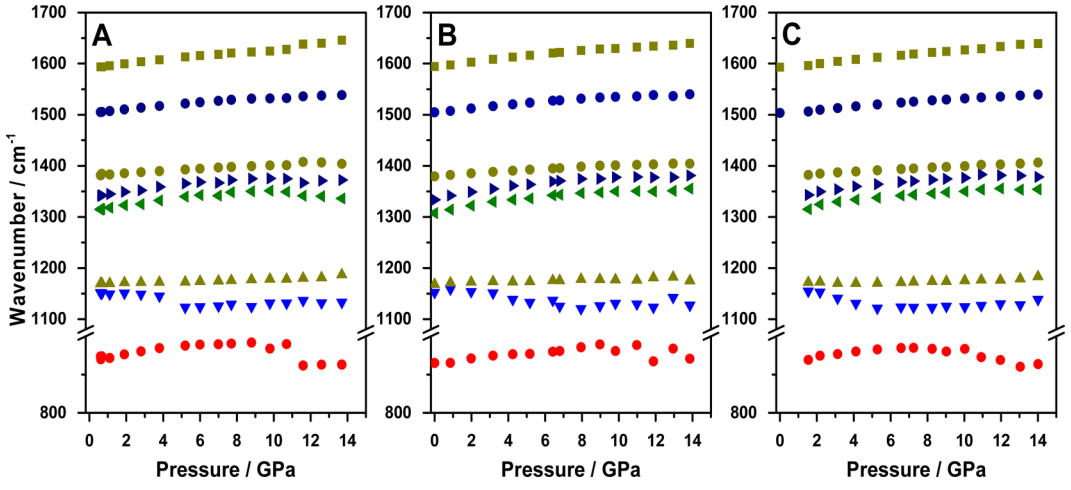

Figure 3. Pressure evolution of the IR modes along compression at 298 K of (A) PANI-EB-bulk, (B) PANI-EB-IF, and (C) PANI-EB-RM.

dx.doi.org/10.1021/jp509154j | J. Phys. Chem. C XXXX, XXX, XXX−XXX

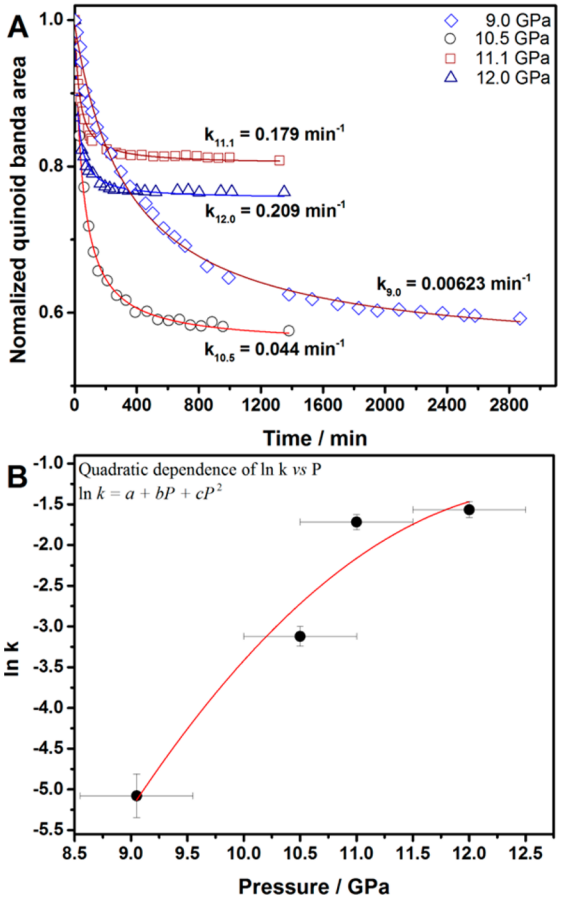

Figure 4. (A) Time evolution of the integrated area of the quinoid band (1595 cm^{-1}) at 9.0 GPa (open rhombus) 10.5 GPa (open circles), 11.1 GPa (open squares), and 12. 0 GPa (open triangles). The rate constant for each pressure in presented in the figure. (B) Quadratic fit of the ln k as a function of pressure at ambient temperature (298 K).

According to these results, the pressure increase favors the reaction by increasing the rate constant. However, a decrease in the amount of reacted quinoid ring ranging from about 40% at 10 GPa to about 20% at 12 GPa (Figure 4A) it is also noticed. This could be due to an increasing steric hindrance with pressure, which reduces the mobility of the polymeric chains preventing the correct geometrical approach of the adjacent chains to give rise to the quinoid rings coupling.

The activation volume of the reaction ($\Delta V^{\ddagger}$), according to the transition state theory, was determined according to the relation of the rate constant and pressure, given by eq 2

$$\left(\frac{\partial \ln k}{\partial P}\right)_T = -\frac{\Delta V^{\ddagger}}{RT} \tag{2}$$

Accordingly, ln k should evolve linearly with pressure, but its nonlinear dependence as a function of pressure is clearly seen from the data presented in Figure 4B. This occurrence is quite common because linear pressure evolution is observed only for small pressure ranges where $\Delta V^{\ddagger}$ can be assumed pressure independent. Usually, the relation of ln k vs pressure can be described by a quadratic function as that presented in the figure. To fit the data, we have used $a = -46.78$, $b = 7.13$, and $c = -0.28$. Using the quadratic relation, the activation volume at any pressure is obtained by eq 3

$$\Delta V^{\ddagger} = -(b + 2cP)RT \tag{3}$$

According to the quadratic dependence of the ln k vs pressure, an inversion in the sign of the activation volume, $\Delta V^{\ddagger}$, from negative (-5.2 cm^3 mol^{-1} at 9 GPa) to positive (1.8 cm^3 mol^{-1} at 14 GPa), is expected at about 13 GPa. This result suggests that as the pressure increases the hindrance of the system is enhanced in such a way that the reaction is not more favored due to the restricted mobility of the polymeric chains. In this case the reaction occurs only in the sites that present the specific orientation of the chains, in accordance to that discussed in Figure 4A.

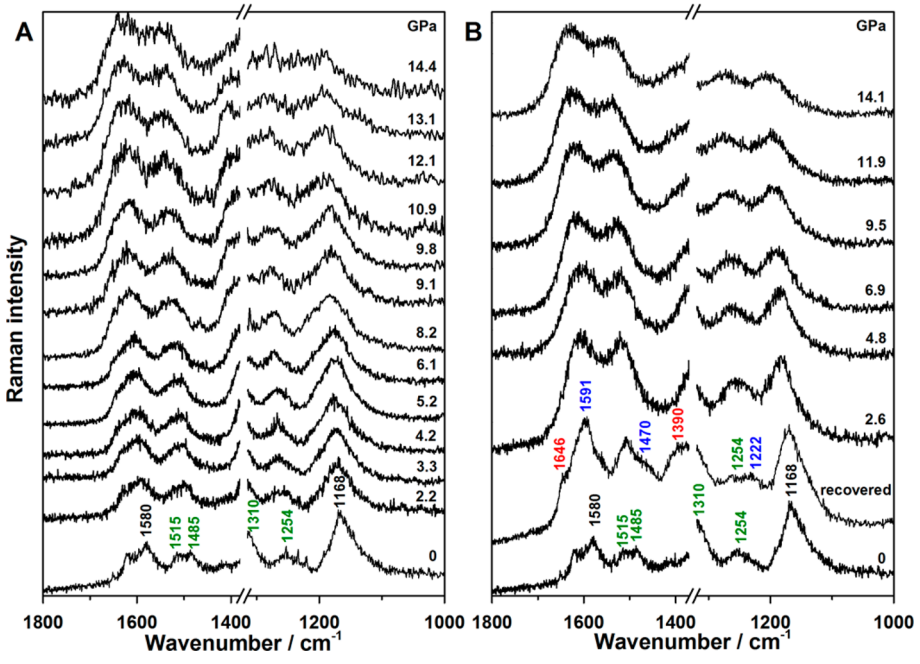

Figure 5. Raman spectra of PANI-ES-IF (A) compression and (B) decompression at 298 K.

dx.doi.org/10.1021/jp509154j | J. Phys. Chem. C XXXX, XXX, XXX−XXX

Raman Spectra. Raman experiments were performed for PANI-EB and PANI-ES with bulk and fiber morphology along a compression−decompression cycle up to 15 GPa. These results are in agreement with the FTIR spectroscopy data. Since the quinoid rings of PANI-EB present a strong resonance condition with the exciting radiation at 647.1 nm, no other changes of polymeric segments during the compression−decompression cycle could be observed (see Supporting Information, Raman spectra).

For PANI-ES-IF, Figure 5 presents the Raman spectra measured during the compression (A)−decompression (B) at ambient pressure with the characteristic bands of the polaronic segments at 1168 (β_{C-H}), 1514 (ν_{C-C}), 1581 (ν_{C-C}) and a shoulder at 1310 ($\nu_{C-N\bullet+}$) cm^{-1} (Figure 5A, bottom spectrum).[54−56] As the pressure increases, a broadening and a blue shift of the bands precede the almost completely lost spectral features observed at about 14 GPa, indicating a partial or complete amorphization of the polymer at this pressure. During the decompression cycle (Figure 5B) some spectral features were recovered and, considering the recovered PANI-ES spectrum, it is noticed the appearance of some bands at 1227, 1460, and 1591 cm^{-1}, which are characteristic of the dedoped form of PANI (PANI-EB),[54−56] and the bands at 1395 and 1645 cm^{-1}, due to the phenazine-like segments.[49,57−63] These results suggest that pressure induces a reversible amorphization of PANI-ES but also that some minor reactions are occurring under high pressure, such as, dedoping and cross-linking formation.

The Raman results for the doped and dedoped forms of PANI with the bulk (PANI-bulk) and fiber morphology (PANI-RM) are briefly discussed in the Supporting Information (see Supporting Information, Raman spectra).

CONCLUSIONS

FTIR and Raman spectra as a function of pressure showed a pressure driven reaction for PANI-EB starting at about 9 GPa. This behavior is independent of the polymeric morphology since the reaction threshold was the same for the polymers with bulk and fiber morphologies. The reaction occurs through the coupling of two quinoid rings, leading to a three condensed ring segment. The reaction kinetics at four pressures (9.0, 10.5 11.1, and 12.0 GPa) showed that with increasing pressure the rate constant increases; however, a decrease in the amount of reacted quinoid ring was also observed as the pressure increases, which could be due to the steric hindrance of the system that prevents an ordering of the chains. The activation volume presented an inversion in its sign, being negative from atmospheric pressure until 9 GPa and positive form this pressure until 14 GPa, suggesting that increasing pressure increases the hindrance of the system and the reaction occurs only in the sites that presents the specific orientation of the chains which were formed during the compression step of the system. Raman data suggested the occurrence of the dedoping and cross-linking reactions after the decompression of the system.

PANI presented a great stability under high pressure, and the possibility to control the chemical structure by tuning the pressure may be a promising tool to optimize the properties of this fascinating material for use in several devices.

ASSOCIATED CONTENT

Supporting Information

Raman spectra of PANI-ES and PANI-EB with bulk and fiber morphologies during the compression and decompression cycle up to 15 GPa at 298 K. This material is available free of charge via the Internet at http://pubs.acs.org.

AUTHOR INFORMATION

Corresponding Author

*Tel.: + 55 11 3091 3890. Fax: + 55 11 3091 3890. E-mail: mlatempe@iq.usp.br.

Notes

The authors declare no competing financial interest.

ACKNOWLEDGMENTS

We thank the Brazilian agencies CNPq and FAPESP (Grant Nos. 2010/18107-8 and 2013/05983-2) for fellowships and financial support.

REFERENCES

(1) Bridgman, P. W. Recent Work in the Field of High Pressures. *Rev. Mod. Phys.* **1946**, *18* (1), 1−93.
(2) Weir, C. E.; Lippincott, E. R.; Valkenburg, A. V.; Bunting, J. Infrared Studies in the 1- to 15-Micron Region to 30000 atm. *J. Res. Natl. Bur. Stand., Sect. A* **1959**, *63A*, 275.
(3) Schettino, V.; Bini, R. Molecules under Extreme Conditions: Chemical Reactions at High Pressure. *Phys. Chem. Chem. Phys.* **2003**, *5* (10), 1951−1965.
(4) Schettino, V.; Bini, R. Constraining Molecules at the Closest Approach: Chemistry at High Pressure. *Chem. Soc. Rev.* **2007**, *36* (6), 869−880.
(5) Schettino, V.; Bini, R.; Cardini, G.; Ceppatelli, M.; Citroni, M.; Pagliai, M. Spectroscopy and Monitoring of High Pressure Phenomena. *J. Mol. Struct.* **2009**, *924−26*, 2−8.
(6) Scelta, D.; Ceppatelli, M.; Santoro, M.; Bini, R.; Gorelli, F. A.; Perucchi, A.; Mezouar, M.; van der Lee, A.; Haines, J. High Pressure Polymerization in a Confined Space: Conjugated Chain/Zeolite Nanocomposites. *Chem. Mater.* **2014**, *26* (7), 2249−2255.
(7) Ceppatelli, M.; Bini, R. Light-Induced Catalyst and Solvent-Free High Pressure Synthesis of High Density Polyethylene at Ambient Temperature. *Macromol. Rapid Commun.* **2014**, *35* (8), 787−793.
(8) Ciabini, L.; Santoro, M.; Bini, R.; Schettino, V. High Pressure Photoinduced Ring Opening of Benzene. *Phys. Rev. Lett.* **2002**, *88* (8), 085505.
(9) Rao, R.; Sakuntala, T.; Godwal, B. K. Evidence for High-Pressure Polymorphism in Resorcinol. *Phys. Rev. B* **2002**, *65* (5), 054108.
(10) Citroni, M.; Ceppatelli, M.; Bini, R.; Schettino, V. The High-Pressure Chemistry of Butadiene Crystal. *J. Chem. Phys.* **2003**, *118* (4), 1815−1820.
(11) Pravica, M. G.; Shen, Y. R.; Nicol, M. F. High Pressure Raman Spectroscopic Study of Structural Polymorphism in Cyclohexane. *Appl. Phys. Lett.* **2004**, *84* (26), 5452−5454.
(12) Ciabini, L.; Gorelli, F. A.; Santoro, M.; Bini, R.; Schettino, V.; Mezouar, M. High-Pressure and High-Temperature Equation of State and Phase Diagram of Solid Benzene. *Phys. Rev. B* **2005**, *72* (9), 094108.
(13) Zeng, Q. G.; Ding, Z. J.; Tang, X. D.; Zhang, Z. M. Pressure Effect on Photoluminescence and Raman Spectra of PPV. *J. Lumin.* **2005**, *115* (1−2), 32−38.
(14) Fabbiani, F. P. A.; Allan, D. R.; Parsons, S.; Pulham, C. R. Exploration of the High-Pressure Behaviour of Polycyclic Aromatic Hydrocarbons: Naphthalene, Phenanthrene and Pyrene. *Acta Crystallogr. B* **2006**, *62*, 826−842.
(15) Ciabini, L.; Santoro, M.; Gorelli, F. A.; Bini, R.; Schettino, V.; Raugei, S. Triggering Dynamics of the High-Pressure Benzene Amorphization. *Nat. Mater.* **2007**, *6* (1), 39−43.

(16) Citroni, M.; Ceppatelli, M.; Bini, R.; Schettino, V. Dimerization and Polymerization of Isoprene at High Pressures. *J. Phys. Chem. B* **2007**, *111* (15), 3910−3917.
(17) Citroni, M.; Datchi, F.; Bini, R.; Di Vaira, M.; Pruzan, P.; Canny, B.; Schettino, V. Crystal Structure of Nitromethane up to the Reaction Threshold Pressure. *J. Phys. Chem. B* **2008**, *112* (4), 1095−1103.
(18) Faria, L. F. O.; Nobrega, M. M.; Temperini, M. L. A.; Ribeiro, M. C. C. Ionic Liquids Based on the Bis(trifluoromethylsulfonyl)imide Anion for High-Pressure Raman Spectroscopy Measurements. *J. Raman Spectrosc.* **2013**, *44* (3), 481−484.
(19) Bhadra, S.; Khastgir, D.; Singha, N. K.; Lee, J. H. Progress in Preparation, Processing and Applications of Polyaniline. *Prog. Polym. Sci.* **2009**, *34* (8), 783−810.
(20) Ćirić-Marjanović, G. Recent Advances in Polyaniline Research: Polymerization Mechanisms, Structural Aspects, Properties and Applications. *Synth. Met.* **2013**, *177* (0), 1−47.
(21) Huang, J. X.; Virji, S.; Weiller, B. H.; Kaner, R. B. Polyaniline Nanofibers: Facile Synthesis and Chemical Sensors. *J. Am. Chem. Soc.* **2003**, *125* (2), 314−315.
(22) Hangarter, C. M.; Bangar, M.; Mulchandani, A.; Myung, N. V. Conducting Polymer Nanowires for Chemiresistive and FET-Based Bio/Chemical Sensors. *J. Mater. Chem.* **2010**, *20* (16), 3131−3140.
(23) Virji, S.; Huang, J. X.; Kaner, R. B.; Weiller, B. H. Polyaniline Nanofiber Gas Sensors: Examination of Response Mechanisms. *Nano Lett.* **2004**, *4* (3), 491−496.
(24) Janata, J.; Josowicz, M. Conducting Polymers in Electronic Chemical Sensors. *Nat. Mater.* **2003**, *2* (1), 19−24.
(25) Ponzio, E. A.; Benedetti, T. M.; Torresi, R. M. Electrochemical and Morphological Stabilization of V_2O_5 Nanofibers by the Addition of Polyaniline. *Electrochim. Acta* **2007**, *52* (13), 4419−4427.
(26) Varela, H.; Huguenin, F.; Malta, M.; Torresi, R. M. Materials for Cathodes of Secondary Lithium Batteries. *Quim. Nova* **2002**, *25* (2), 287−299.
(27) Venkatachalam, S.; Prabhakaran, P. V. Oligomeric Phthalocyanine Modified Polyaniline - an Electrode Material for Use in Aqueous Secondary Batteries. *Synth. Met.* **1998**, *97* (2), 141−146.
(28) Nobrega, M. M.; Souza, K. S.; Andrade, G. F. S.; Camargo, P. H. C.; Temperini, M. L. A. Emeraldine Salt Form of Polyaniline As a Probe Molecule for Surface Enhanced Raman Scattering Substrates Excited at 1064 nm. *J. Phys. Chem. C* **2013**, *117* (35), 18199−18205.
(29) Barbero, C.; Miras, M. C.; Schnyder, B.; Hass, O.; Kotz, R. Sulfonated Polyaniline Films As Cation Insertion Electrodes for Battery Applications. Part 1. Structural and Electrochemical Characterization. *J. Mater. Chem.* **1994**, *4* (12), 1775−1783.
(30) Li, P.; Tan, T. C.; Lee, J. Y. Corrosion Protection Of Mild Steel By Electroactive Polyaniline Coatings. *Synth. Met.* **1997**, *88* (3), 237−242.
(31) Nobrega, M. M.; Martins, V. L.; Torresi, R. M.; Temperini, M. L. A. One-Step Synthesis, Characterization, and Properties of Emeraldine Salt Nanofibers Containing Gold Nanoparticles. *J. Phys. Chem. C* **2014**, *118* (8), 4267−4274.
(32) Gu, D. W.; Li, J. S.; Liu, J. L.; Cai, Y. M.; Shen, L. J. Polyaniline Thin Films In Situ Polymerized under Very High Pressure. *Synth. Met.* **2005**, *150* (2), 175−179.
(33) Li, J. S.; Shen, L. J.; Gu, D. W.; Yuan, P. F.; Cui, X. B.; Yang, N. R. Optimum Conditions for the Preparation of Polyaniline Films under Very High Pressure. *React. Funct. Polym.* **2006**, *66* (11), 1319−1326.
(34) Bao, Z. X.; Colon, F.; Pinto, N. J.; Liu, C. X. Pressure Dependence of the Resistance in Polyaniline and Poly(*O*-toluidine) at Room Temperature. *Synth. Met.* **1998**, *94* (2), 211−213.
(35) Bao, Z. X.; Liu, C. X.; Pinto, N. J. Electrical Conductivity of Polyaniline As a Function of Pressure Using a Diamond Anvil Cell. *Synth. Met.* **1997**, *87* (2), 147−150.
(36) Zeng, X. R.; Gong, K. C.; Weng, K. N.; Xiao, W. S.; Gan, W. H.; Ko, T. M. Effects of Ultra-High Pressures (>3.6 GPa) on the Electrical Resistance of Polyaniline by In Situ FT-IR Studies. *Chem. Phys. Lett.* **1997**, *280* (5−6), 469−474.
(37) Chen, C. H. Thermal and Morphological Studies of Chemically Prepared Emeraldine-Base-Form Polyaniline Powder. *J. Appl. Polym. Sci.* **2003**, *89* (8), 2142−2148.
(38) Luo, K.; Shi, N. L.; Sun, C. Thermal Transition Of Electrochemically Synthesized Polyaniline. *Polym. Degrad. Stab.* **2006**, *91* (11), 2660−2664.
(39) Mathew, R.; Mattes, B. R.; Espe, M. P. A Solid State NMR Characterization of Cross-Linked Polyaniline Powder. *Synth. Met.* **2002**, *131* (1−3), 141−147.
(40) Nobrega, M. M.; Silva, C. H. B.; Constantino, V. R. L.; Temperini, M. L. A. Spectroscopic Study on the Structural Differences of Thermally Induced Cross-Linking Segments in Emeraldine Salt and Base Forms of Polyaniline. *J. Phys. Chem. B* **2012**, *116* (48), 14191−14200.
(41) Tsukruk, V. V. Assembly of Supramolecular Polymers in Ultrathin Films. *Prog. Polym. Sci.* **1997**, *22* (2), 247−311.
(42) Prokes, J.; Varga, M.; Krivka, I.; Rudajevova, A.; Stejskal, J. The Influence of Compression Pressure on Transport Properties of Polyaniline. *J. Mater. Chem.* **2011**, *21* (13), 5038−5045.
(43) Zhang, D. On the Conductivity Measurement of Polyaniline Pellets. *Polym. Test.* **2007**, *26* (1), 9−13.
(44) Huang, J.; Wan, M. Temperature and Pressure Dependence of Conductivity of Polyaniline Synthesized by in Situ Doping Polymerization in the Presence of Organic Function Acid As Dopants. *Solid State Commun.* **1998**, *108* (4), 255−259.
(45) MacDiarmid, A. G.; Chiang, J. C.; Richter, A. F. *Conducting Polymers*; Riedel Publications: Dordrecht, 1987; p 105.
(46) Huang, J.; Kaner, R. B. Nanofiber Formation in the Chemical Polymerization of Aniline: A Mechanistic Study. *Angew. Chem., Int. Ed.* **2004**, *43* (43), 5817−5821.
(47) Mao, H. K.; Bell, P. M.; Shaner, J. W.; Steinberg, D. J. Specific Volume Measurements Of Cu, Mo, Pd, and Ag and Calibration of the Ruby R1 Fluorescence Pressure Gauge From 0.06 to 1 Mbar. *J. Appl. Phys.* **1978**, *49* (6), 3276−3283.
(48) da Silva, J. E. P.; Temperini, M. L. A.; de Torresi, S. I. C. Secondary Doping of Polyaniline Studied by Resonance Raman Spectroscopy. *Electrochim. Acta* **1999**, *44* (12), 1887−1891.
(49) da Silva, J. E. P.; de Faria, D. L. A.; de Torresi, S. I. C.; Temperini, M. L. A. Influence of Thermal Treatment on Doped Polyaniline Studied by Resonance Raman Spectroscopy. *Macromolecules* **2000**, *33* (8), 3077−3083.
(50) Izumi, C. M. S.; Constantino, V. R. L.; Temperini, M. L. A. Polyaniline/Layered Zirconium Phosphate Nanocomposites: Secondary-Like Doped Polyaniline Obtained by the Layer-by-Layer Technique. *J. Nanosci. Nanotechnol.* **2007**, *8* (4), 1782−1789.
(51) Lee, K.; Heeger, A. J.; Cao, Y. Reflectance Spectra of Polyaniline. *Synth. Met.* **1995**, *72* (1), 25−34.
(52) MacDiarmid, A. G.; Epstein, A. J. The Concept of Secondary Doping as Applied to Polyaniline. *Synth. Met.* **1994**, *65* (2−3), 103−116.
(53) Boyer, M. I.; Quillard, S.; Rebourt, E.; Louarn, G.; Buisson, J. P.; Monkman, A.; Lefrant, S. Vibrational Analysis of Polyaniline: A Model Compound Approach. *J. Phys. Chem. B* **1998**, *102* (38), 7382−7392.
(54) Furukawa, Y.; Ueda, F.; Hyodo, Y.; Harada, I.; Nakajima, T.; Kawagoe, T. Vibrational-Spectra and Structure of Polyaniline. *Macromolecules* **1988**, *21* (5), 1297−1305.
(55) Louarn, G.; Lapkowski, M.; Quillard, S.; Pron, A.; Buisson, J. P.; Lefrant, S. Vibrational Properties Of Polyaniline - Isotope Effects. *J. Phys. Chem.* **1996**, *100* (17), 6998−7006.
(56) Gruger, A.; Novak, A.; Regis, A.; Colomban, P. Infrared and Raman-Study of Polyaniline 0.2. Influence of Ortho Substituents on Hydrogen-Bonding and UV/Vis near-Ir Electron Charge-Transfer. *J. Mol. Struct.* **1994**, *328*, 153−167.
(57) Do Nascimento, G. M.; Constantino, V. R. L.; Landers, R.; Temperini, M. L. A. Aniline Polymerization into Montmorillonite Clay: A Spectroscopic Investigation of the Intercalated Conduct-Ling Polymer. *Macromolecules* **2004**, *37* (25), 9373−9385.
(58) Do Nascimento, G. M.; da Silva, J. E. P.; de Torresi, S. I. C.; Temperini, M. L. A. Comparison of Secondary Doping and Thermal

Treatment in Poly(diphenylamine) and Polyaniline Monitored by Resonance Raman Spectroscopy. *Macromolecules* **2002**, *35* (1), 121−125.

(59) Do Nascimento, G. M.; Silva, C. H. B.; Izumi, C. M. S.; Temperini, M. L. A. The Role of Cross-Linking Structures to the Formation of One-Dimensional Nano-Organized Polyaniline and Their Raman Fingerprint. *Spectrochim. Acta, Part A* **2008**, *71* (3), 869−875.

(60) Do Nascimento, G. M.; Silva, C. H. B.; Temperini, M. L. A. Spectroscopic Characterization of the Structural Changes of Polyaniline Nanofibers after Heating. *Polym. Degrad. Stab.* **2008**, *93* (1), 291−297.

(61) Ciric-Marjanovic, G.; Trchova, M.; Stejskal, J. The Chemical Oxidative Polymerization of Aniline in Water: Raman Spectroscopy. *J. Raman Spectrosc.* **2008**, *39* (10), 1375−1387.

(62) Sedenkova, I.; Trchova, M.; Stejskal, J. Thermal Degradation of Polyaniline Films Prepared in Solutions of Strong and Weak Acids and in Water - FTIR and Raman Spectroscopic Studies. *Polym. Degrad. Stab.* **2008**, *93* (12), 2147−2157.

(63) Wu, L. L.; Luo, J.; Lin, Z. H. Spectroelectrochemical Studies Of Poly-*O*-phenylenediamine 0.1. In Situ Resonance Raman Spectroscopy. *J. Electroanal. Chem.* **1996**, *417* (1−2), 53−58.